In-plane intercalate lattice modes in graphite-bromine using Raman spectroscopy

P. C. Eklund,*†‡ N. Kambe,* G. Dresselhaus,§ and M. S. Dresselhaus*†
Massachusetts Institute of Technology, Cambridge, Massachusetts 02139
(Received 23 January 1978)

Results of Raman scattering experiments associated with in-plane intercalate modes in graphite-bromine are reported. The spectra are interpreted in terms of models in which the molecular character of the bromine is retained and the molecular ordering of the intercalate layer is closely related to that in the layer structure of solid molecular bromine. The symmetry and group-theoretical analysis of several possible molecular arrangements are given. A large resonant enhancement of the Br_2 stretch mode is reported, which suggests molecular excitations for intercalated Br_2 at energies $\gtrsim 2.8$ eV.

I. INTRODUCTION

On the basis of various experiments sensitive to the electronic[1-4] and crystal[5,6] structure, it has been inferred that bromine retains its molecular identity when intercalated into graphite-bromine compounds $C_{8n}Br_2$, in which the stage is denoted by n, and n has values $n \geq 2$. These conclusions follow from infrared and far-infrared magnetoreflection studies,[1] Hall-effect measurements,[1,2] optical-reflectivity studies in the vicinity of the plasma edge,[3,4] and x-ray and electron-diffraction studies.[5,6] The common feature of all the electronic techniques is their primary sensitivity to carriers associated with the ionized species rather than to the neutral molecules themselves. More specifically, these experiments provide evidence for small shifts in the Fermi level (or changes in carrier concentration) per unit increment in bromine intercalate concentration. In the case of the x-ray and electron diffraction studies, the great similarities between the intramolecular and intermolecular bromine-bromine distances in graphite-bromine compounds and in solid bromine (a molecular solid) provide additional support for the molecular identity of bromine in the graphite-bromine compounds.[5,6]

In contrast, Raman-scattering studies are directly sensitive to the molecular species, insofar as spectral features specific to the molecular intercalate species have been identified in graphite-bromine.[7] In the present paper, the lattice-mode structure of graphite-bromine is explored in more detail. Of particular interest is the first observation of a resonant enhancement effect associated with the electronic states of the intercalate species. This may have interesting implications for the applications of Raman spectroscopy to the study of other intercalate species.

Previous studies of the Raman spectra of graphite intercalation compounds[7-11] have emphasized spectral features identified with in-plane lattice modes due to carbon-atom vibrations. The characteristics of the spectral features identified with the in-plane graphite modes have been interpreted to imply that the in-plane force constants in the graphitic-layer planes are essentially unaffected by intercalation for *interior* graphite layers (*not adjacent* to intercalate layer planes), and are only slightly affected for *bounding* graphitic layers (*adjacent* to intercalate layer planes). These conclusions follow from the following observations and arguments. In graphite-bromine, as in almost all graphite intercalation compounds studied to date, a Raman doublet is observed near the E_{2g_2} mode of pristine graphite.[7,8,10] The lower-frequency component of the doublet structure is characteristically found at 1582 cm^{-1}, essentially unshifted from its position in pristine graphite, and with an intensity which decreases with increasing bromine concentration. In contrast, the upper frequency component, not present in pristine graphite is characteristically upshifted by ~20 cm^{-1}, and has an intensity which increases with increasing intercalate concentration. Consequently, the lower-frequency component has been identified with an E_{2g_2}-type mode for interior graphite layers, while the upper-frequency component has been attributed to a similar mode occurring in the bounding graphite planes. Thus the graphitic layers in the graphite-bromine compounds are closely related to graphite layers in pristine graphite.[12]

Correspondingly, it might be expected that the intercalate layers in the graphite-bromine compounds are closely related to layers in the parent molecular solid Br_2.[10] The dominant Raman-active in-plane mode in solid Br_2 is the stretching mode of the bromine molecules at ~300 cm^{-1}.[13] This frequency is downshifted from 323 cm^{-1} for the free Br_2 molecules[14] because of intermolecular Br_2 interactions. In a preliminary account of the Raman spectrum of graphite bromine, a strong line at ~242 cm^{-1} was identified with the stretching mode of Br_2 in the intercalation compounds

$C_{8n}Br_2$.[7] Of the various techniques which have thus far been applied to the study of graphite intercalation compounds, Raman spectroscopy is the only technique which provides specific information on each of the types of layer planes which occur in graphite intercalation compounds: *interior graphite* layers, *bounding graphite* layers, and *intercalate* layers.

The major objective of this paper is to present further details on the spectra associated with the bromine intercalate. Particular emphasis is given to the relation between information on the intercalate species provided by in-plane intercalate lattice modes and by other experimental techniques.

In Sec. II, we discuss structural considerations in terms of the molecular identity of the bromine intercalate. On the basis of these structural considerations, some model lattice modes for graphite-bromine are suggested. In Sec. III, experimental details relevant to the Raman experiment are summarized and in Sec. IV the experimental Raman results are presented. A brief discussion is given of the relation between deductions based on the Raman spectra and on other experimental techniques.

II. STRUCTURAL CONSIDERATIONS

In this paper emphasis is given to the lattice modes which are identified with the intercalate layer of the graphite-bromine intercalation compounds. It is of particular significance to the interpretation of the Raman spectra that the crystal structure of the intercalate layer is very similar to that of the parent compound, solid bromine.

Bromine crystallizes[15] below 265.9 K in an orthorhombic molecular solid (space group V_h^{18}). In this solid, the bromine molecules lie with their molecular axes aligned in layer planes with lattice constants $a_{Br} = 4.48$ Å and $b_{Br} = 8.72$ Å (see Fig. 1). The stability of the $C_{8n}Br_2$ intercalation compound may well be due to the fact that, by only a slight distortion, the layer planes in solid bromine can be made commensurate with those of pristine graphite. This approximate registry is illustrated in Fig. 1 where the layer plane of solid bromine is projected on to the graphite-layer plane. In particular, the in-plane lattice constants of solid bromine are similar to those of the C_8X Rüdorff structure[16] where an intercalate unit, X, would be located at the center of each of the hexagons containing Br_2 molecules in Fig. 1. The small distortions of the solid-Br_2 in-plane unit cell required to achieve registry with this C_8X structure are $a_X = 4.91$ Å and $b_X = 8.50$ Å as shown in Fig. 1. Not only are the in-plane lattice constants similar but also the interlayer distances of solid bromine and pristine graphite are similar, with 3.35 Å for graphite and 3.33 Å for solid Br_2. These similarities in the various lattice constants suggest that the introduction of a bromine layer between two graphite layers should have only a minor effect on the in-plane force constants for both the bromine and bounding graphite layers, and a negligible effect on the interior graphite layers.

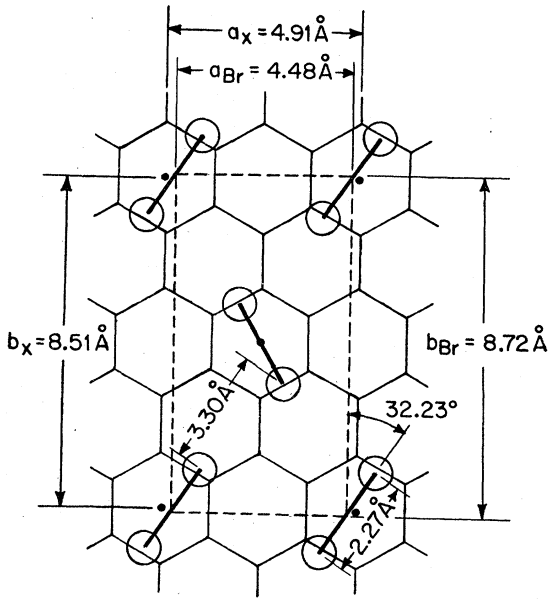

FIG. 1. Projection of a lattice plane of solid Br_2 on the hexagonal graphite network. The dashed lines indicate the unit cell for solid Br_2, and the molecular axes lie in this lattice plane. This figure shows that with only slight displacement of the Br_2 molecules, the center-of-mass positions of the intercalate species can be placed on C_8X intercalate sites (small closed circles). However, this ordering of the Br_2 axes does not exhibit the threefold symmetry of graphite. In this figure the dimensions of the unit cell for solid bromine a_{Br}, b_{Br} are given as well as the dimensions of the unit cell required to achieve registry with the graphite network a_X, b_X. The intramolecular and intermolecular bromine distances and axis orientation are also indicated.

Analyses of x-ray and electron diffraction patterns[5,6] further show that when bromine is intercalated into graphite, the nearest-neighbor Br-Br distance is in a layer plane and is equal to 2.27 Å, which is the same as the intramolecular Br-Br distance in solid bromine and in the gas phase. This observation provides strong support for the molecular identity of the Br_2 intercalate and for the close association of the intercalate bromine layer with the corresponding layer in the parent molecular solid bromine. It is also of interest to note that this intramolecular distance of 2.27 Å is comparable with the "altitude" of the graphite hexagons which is 2.46 Å. From these geometric con-

siderations it follows that the two bromine atoms of a single molecule can conveniently lie over adjacent hexagons.

Analyses of x-ray data sensitive to c-axis lattice constants for the graphite-bromine intercalation compounds have been interpreted in terms of a thickness of 3.69 Å for the bromine intercalate layer.[17] This increase in thickness from 3.33 Å for solid bromine suggests that the interlayer intercalate-graphite binding energy is weaker than that in either of the parent compounds. This conclusion is also consistent with the decrease in c-axis conductivity upon intercalation of bromine into graphite.[18,19]

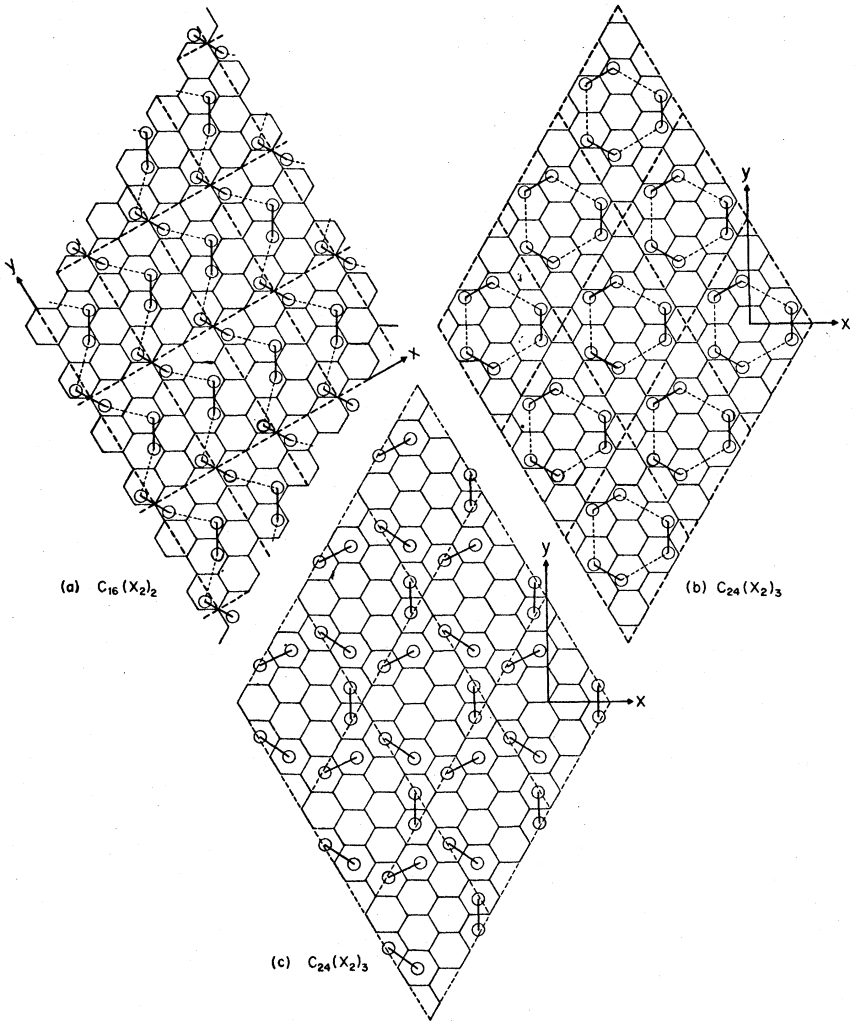

FIG. 2. Models for layer structure of graphite-bromine intercalate compounds. (a) To obtain this model from Fig. 1, the center of masses of the Br_2 molecules are placed in a unit cell commensurate with the C_8X structure, and the intercalate structure is rigidly displaced relative to the graphite structure by a distance equal to the side of a graphite hexagon. In this figure, the intramolecular Br-Br distance is the same as in solid and gaseous bromine. Intercalate chains are formed by following the bromine atoms with minimum separations. Between the intercalate chains are unoccupied channels. [The intramolecular distances (2.27 Å) are indicated by solid lines and the nearest-neighbor intermolecular distances (3.36 Å) are indicated by dashed lines.] (b) This model is for a commensurate graphite-bromine structure which exhibits threefold symmetry. Each unit cell, denoted by the dashed lines, contains three Br_2 molecules and 24 carbon atoms in each layer plane. In this arrangement, the bromine molecules form islands and the unoccupied hexagons form chains. The nearest-neighbor intermolecular distance for bromine atoms on adjacent hexagons is 3.78 Å (dashed line) while the intramolecular and nearest-neighbor intermolecular distances are 2.27 and 3.36 Å, respectively. (c) This model is for a commensurate graphite-bromine structure which exhibits threefold symmetry. Each unit cell, denoted by the dashed lines, contains three Br_2 molecules and 24 carbon atoms in each layer plane. In this arrangement, the bromine atoms are arranged on chains which are cross-linked to each other, enclosing an island of six unoccupied hexagons. The intramolecular and nearest-neighbor intermolecular distances are 2.27 and 3.36 Å, respectively.

The basic point group symmetry of an isolated graphite layer is D_{6h} and that of a layer in solid bromine is D_{2h}. As shown in Fig. 1, a unit cell in solid bromine contains two Br_2 molecules. However, the in-plane arrangement of the bromine molecules in the intercalation compound has not been fully established.

One possible arrangement of the bromine molecules in the intercalation compound is shown in Fig. 2(a). This arrangement is obtained from that in solid bromine by a small in-plane distortion of the bromine layer to make it commensurate with the graphite layer, and by a displacement of the origin of the unit cell in Fig. 1 to increase the bromine-carbon (interplanar) distances and to yield a symmetric molecular configuration. The arrangement in Fig. 2(a) has C_{2v} symmetry and the unit cells are denoted by the heavy dashed lines, each containing two Br_2 molecules, thereby corresponding to the chemical formula $C_{16}(X_2)_2$ for a single graphite layer and a single intercalate layer (a hypothetical stage-1 compound). The symmetry operations in Fig. 2(a) include a twofold axis in the y direction followed by a translation, an xy reflection plane, and a yz reflection plane combined with a translation. It is significant that this structure does not contain a threefold axis, the most characteristic symmetry operation of graphitic structures. By considering molecular arrangements on neighboring intercalate layers, a threefold screw axis can be introduced through a three-layer intercalate sequence in which each layer is rotated by $\frac{2}{3}\pi$ relative to the adjacent intercalate layer; in this case, the real-space unit cell would be correspondingly enlarged.

Returning to the layer plane network of Fig. 2(a) it is seen that the bromine molecules are arranged in chains, with each link containing three bromine atoms, having an intramolecular Br-Br distance of 2.27 Å and an intermolecular Br-Br distance of 3.36 Å. Between the chains are channels. An alternate chain arrangement for the bromine intercalate was first proposed by Eeles and Turnbull[5,6] to explain their x-ray and electron diffraction patterns. Although they were unable to explain their experimental patterns in detail, their results clearly provide evidence for the molecular identity of the bromine intercalate, for Br_2 molecular axes aligned within the layer planes and for a chainlike intercalate arrangement. Their work shows that the intramolecular Br-Br distance is essentially unchanged upon intercalation, and a commensurate intercalation compound is achieved by distortion of the intermolecular Br-Br distance to establish registry between the arrangements on the intercalate and graphite-layer planes.[5,6] Evidence for this registry comes from both the magnitudes of the intramolecular and intermolecular Br-Br distances and the absence of superlattice structures due to incommensurate multiple-electron-diffraction spots. The electron-diffraction patterns obtained by Eeles and Turnbull, and those latter obtained by Chung,[20] suggest a large real-space unit cell. But there are problems associated with the chain structure as proposed by Eeles and Turnbull in making it compatible with the $C_{8n}Br_2$ chemical formula for a single-phase intercalation compound.

Whereas the molecular arrangement of Fig. 2(a) emphasizes the connection between the graphite-bromine and solid-bromine structures, alternative arrangements shown in Figs. 2(b) and 2(c) emphasize the connection between graphite-bromine and the graphite host crystal by featuring a characteristic threefold symmetry. Here the appropriate symmetry group is D_{3h}. In Fig. 2(b) the planar unit cell marked by the heavy dashed lines contains three bromine molecules and is described by the chemical formula $C_{24}(Br_2)_3$. In addition to the threefold rotations about the z axis, there are three in-plane twofold axes. In the planar structure in Fig. 2(b), the intramolecular Br-Br distance denoted by a solid line in the figure is maintained at 2.27 Å and the smallest intermolecular Br-Br distance required to achieve registry with the graphite layers is 3.36 Å. In the figure, bromine atoms are located above half of the hexagons of the graphite network (denoted here as occupied hexagons), while the other hexagons are correspondingly unoccupied. Each planar unit cell contains an island formed by six bromine atoms enclosing a single unoccupied hexagon. Between these islands are chains of unoccupied hexagons. We note that the nearest neighbor Br-Br intermolecular distance is 3.36 Å, but in this case the two bromine atoms lie in different unit cells and span an unoccupied hexagon. On the other hand, the nearest-neighbor intermolecular Br-Br distance for bromine atoms occupying adjacent hexagons is 3.78 Å (indicated by dashed lines in the figure).

Another arrangement also having D_{3h} symmetry is shown in Fig. 2(c). This arrangement is obtained from Fig. 2(b) by a rigid translation of the intercalate layer along the x direction for a distance equal to the side of a hexagon followed by an expansion of the intercalate hexagon [shown in Fig. 2(b) by the alternate solid and dashed lines] so that the bromine molecules are now centered over sides of the graphite hexagons. Thus, the molecular arrangements in Figs. 2(c) and 2(b) have equivalent symmetry operations. By following bromine atoms contained in adjacent occupied graphite hexagons, it is found that the arrangement of Fig. 2(c) results in chains along three equivalent in-plane directions, in contrast with

the structure in Fig. 2(a) where the chains are arranged in a single direction (the y direction). In Fig. 2(c), a collection of six Br_2 molecules occupy 12 hexagons which surround an island of six unoccupied hexagons. Whereas the arrangement of Fig. 2(a) has chains of both occupied and unoccupied hexagons, the structure of Fig. 2(c) has no chains connecting unoccupied hexagons, but rather has a network of crossing chains connecting occupied hexagons, and these crossing chains are oriented in three equivalent in-plane directions. The molecular arrangements shown in Figs. 2(b) and 2(c) are two examples of a variety of molecular arrangements exhibiting the threefold-symmetry characteristic of the graphite-layer structure.

On the basis of the structural arrangements suggested in Fig. 2(a) for C_{2v} symmetry and Figs. 2(b) and 2(c) for D_{3h} symmetry, the in-plane lattice-mode patterns for zero wave vector can be obtained. The results for these two symmetries are shown, respectively, in Figs. 3(a) and 3(b). Because of the close connections of the symmetries in Figs. 2(b), 2(c), and 3(b), the lattice-mode patterns corresponding to the structures of Figs. 2(b) and 2(c) can be deduced from the patterns shown in Fig. 3(b) by appropriate translation of the Br_2 molecules relative to the graphite honeycomb structure (to be described explicitly below).

For the structure of Fig. 2(a) which has C_{2v} symmetry, there are eight in-plane modes, four having A_1 symmetry and four having B_2 symmetry. These symmetry designations follow the character table in Table I and those given by Cahill and Leroi[13] for the solid-bromine modes which have D_{2h} symmetry. Six of the modes correspond to librations and are denoted in Fig. 3(a) by the subscript l_i, $i=1,2,3$. The remaining two modes correspond to molecular stretch modes and are correspondingly denoted by the subscript s. It is clear from this figure that any displacements of the bromine atoms corresponding to the A_1 modes do not change the symmetry of the molecular arrangement of Fig. 2(a), nor the symmetries of the eight in-plane modes. Thus the modes in Fig. 3(a) are appropriate for all molecular arrangements derived from Fig. 2(a) by bromine-atom displacements with A_1 symmetry; all such derived molecular arrangements will also have C_{2v} symmetry.

The in-plane lattice modes in Fig. 3(a) are expected to occur at approximately the frequency of the corresponding modes in solid bromine,[13] which for the molecular stretch modes are observed at 296.1, 297.4, 299.0 (weak), and 303.2 cm^{-1} (at 15 K) and for the librational modes at 55, 74, 86, and 101 cm^{-1} (at 15 K). In solid bromine the frequency difference between the two molecular stretch modes is comparable in magnitude to the shifts associated with an isotope effect[13] arising

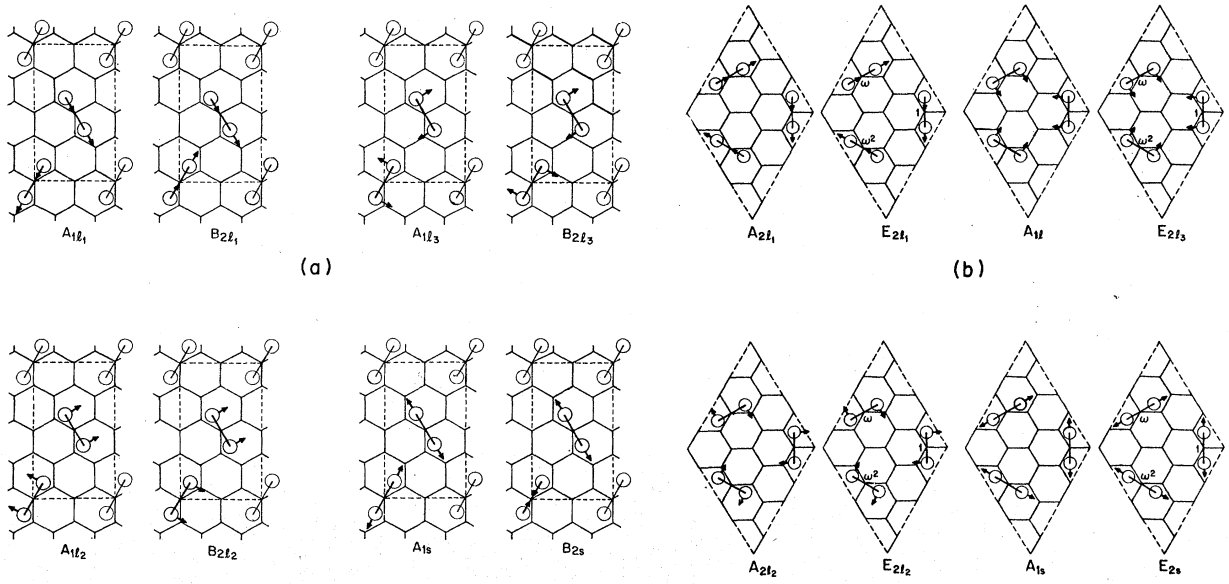

FIG. 3. In-plane intercalate normal modes. (a) The eight in-plane normal modes corresponding to the molecular arrangement in Fig. 2(a) with two bromine molecules per unit cell. The eight modes have symmetries A_1 and B_2 in accordance with Table I and are further classified as librational (l) or molecular stretch modes (s). (b) The 12 in-plane normal modes corresponding to the molecular arrangement in Fig. 2(c) with three bromine molecules per unit cell. The modes are classified by their symmetry designations (A_1, A_2, and E_2) and as librations (l) or molecular stretch modes (s). The displacements for the A_1 and A_2 modes are in phase, while the E_2 modes have displacements with phase differences indicated $\omega = e^{(2\pi i/3)}$ and $\omega^2 = e^{(-2\pi i/3)}$ (see text).

from the presence of ^{79}Br-^{79}Br, ^{79}Br-^{81}Br, and ^{81}Br-^{81}Br isotopic combinations, and occurring with the natural-abundance ratio 1:2:1. In the intercalation compounds, the Raman lines are sufficiently broad so that an isotope splitting has not been identified.

In the case of the structural arrangements with symmetry D_{3h} shown in Figs. 2(b) and 2(c), the in-plane lattice-mode patterns are quite different and are shown in Fig. 3(b). In this case the three molecular units per unit cell, give rise to 12 in-plane lattice modes with symmetries $4E_2+2A_1+2A_2$ (referred to the D_{3h} group). The corresponding normal modes are either librations (labeled l) or molecular stretch modes (labeled s). Subscripts on l are used to distinguish librational modes with similar symmetries. The displacements for the three molecules per unit cell in the A_1 and A_2 modes are all in phase, while for the E_2 modes the displacements of the three molecules have the relative phases $(1, \omega, \omega^2)$ and $(1, \omega^2, \omega)$ corresponding to the two degenerate partners of the E_2 modes where $\omega = e^{2\pi i/3}$. Figure 3(b) shows the E_2 mode for the partner with relative phases $(1, \omega, \omega^2)$.

The following connection is made between the unit cells of Figs. 2(b), 2(c), and 3(b). The unit cell indicated for Fig. 3(b) is identical to that in Fig. 2(b), but differs from that in Fig. 2(c) by a translation along the x axis for a distance $-(1/\sqrt{3})a_{gr}$ ($a_{gr} = 2.46$ Å for the graphite structure). The positions of the bromine molecules within the unit cell in Fig. 2(c) are obtained from those in Fig. 3(b) by a displacement corresponding to an A_{1l} mode. Similarly, displacements corresponding to the A_{1s} mode would not change the symmetry of the molecular arrangement. It is expected that for similar types of molecular vibrations, the in-plane mode frequencies will be approximately equal, independent of whether the structural arrangement corresponds to Figs. 2(a)–2(c) or to solid bromine.

III. EXPERIMENTAL DETAILS

The Raman spectra presented here were taken on c faces of graphite-bromine compounds for a variety of bromine concentrations using the Brewster-angle backscattering geometry. Laser excitation was provided by either an argon or a krypton-ion laser. Low laser powers were used to prevent laser heating effects.[8] The spectra were taken with the incident electric field in the layer planes, so that only in-plane lattice modes were excited. In determining the ratios of the peak intensities as a function of laser excitation energy, corrections for the instrument function were taken into account.

Lamellar graphite-bromine samples of varying intercalate concentrations were prepared in two ways. The second-stage $C_{16}Br_2$ samples were prepared by exposing highly oriented pyrolytic graphite to a saturated atmosphere of bromine vapor for several days at room temperature until equilibrium was achieved, following the methods of Saunders *et al.*[21] and Hennig.[22] Samples with lower bromine concentrations were prepared by immersing the pyrolytic graphite host material into a solution of CCl_4 containing varying concentrations of bromine. In the present application of the solution method, samples were grown slowly (over a period of ~2 weeks), starting from very dilute solutions; the bromine concentration was increased gradually, in steps. The samples were equilibrated at each step until the desired intercalate concentration was achieved. An alternate method for the preparation of high-stage graphite-bromine compounds is that of Sasa *et al.*[23] who used vapor intercalation; with this method, the Br_2 vapor pressure and temperature must be carefully controlled.

The samples were stored in liquid nitrogen to prevent desorption of the intercalate. In preparation for a Raman measurement, the samples were quickly transferred to the optical Dewar under an atmosphere of blowing dry nitrogen. With some practice, this transfer procedure could be carried out in less than 1 min. Inside the optical Dewar, the samples were cooled by nitrogen exchange gas and by conduction to a cold finger in the Dewar. The samples were anchored to the cold finger with spring clips.

The intercalate concentration was determined from the weight taken up by the sample. To check that no intercalate desorption occurred during the

TABLE I. Character table for structure in Fig. 2(a) (C_{2v} symmetry). $\vec{\tau} = \frac{1}{2}(\vec{a}_X + \vec{b}_X)$.

Representation	$(E\|0)$	$(C_2\|\vec{\tau})$	$(\sigma_h\|0)$	$(\sigma_v\|\vec{\tau})$	Basis functions
A_1	1	1	1	1	y, x^2, y^2, z^2
B_1	1	−1	−1	1	z, yz
B_2	1	−1	1	−1	x, xy
B_3	1	1	−1	−1	xz

mounting and measurement procedure, typical samples were weighed just after removal from the storage Dewar at the start of the Raman experiment and just before their return to storage when the Raman experiment was completed.

IV. EXPERIMENTAL RESULTS AND DISCUSSION

The in-plane Raman spectrum from graphite-bromine consists of a high-frequency doublet structure associated with lattice vibrations in the graphite layers and structure at lower frequencies associated with the intercalate layers.[7] The structure associated with the intercalate layers is shown in Fig. 4 for a graphite-bromine compound with 2.7-mole% Br_2 at 77 K. The most pronounced low-frequency feature of this spectrum is the strong broad peak at $\omega_0 = 242$ cm^{-1}. In addition, several harmonics (suggestive of a resonant Raman process) of this line are observed and are denoted in Fig. 4 as $2\omega_0$, $3\omega_0$, $4\omega_0$, and $5\omega_0$. The fundamental at 242 cm^{-1} is downshifted by 58 cm^{-1} from the line with which it is associated in solid bromine.[13] Spectra similar to that shown in Fig. 4 are observed over a wide range of intercalate concentrations, including second-stage $C_{16}Br_2$ with 6.25-mole% Br_2. It is of special significance that the spectrum shown in Fig. 4 is specific to the intercalate bromine and is not observed for other intercalate species. Thus, in this frequency range, the observed spectra are sensitive to the intercalate species.

The structure in the vicinity of ω_0 (see Fig. 4) is broad and quite complicated. This complexity is illustrated in Fig. 5 where the spectrum in the range $90 < \omega < 330$ cm^{-1} is shown on an expanded scale for a stage-2 bromine-saturated sample. The solid curve gives the experimentally observed spectrum, which is fit by several Lorentzian components (shown in Fig. 5 as dashed curves). The frequency at the peak intensity, the linewidths, and the intensity for each component are listed in Table II. The superposition of the dashed curves is given as the dotted curve in Fig. 5 and good agreement with the experimental curve is obtained. The analysis indicated in Fig. 5 shows the spectra to consist of two principal components, with the most intense component at 246.5 cm^{-1} and a second component at 230 cm^{-1}. In terms of the notation in Fig. 4, this analysis yields $\omega_0 = 246.5$ cm^{-1} for a stage-2 compound at 77 K. The shift in ω_0 between Figs. 4 and 5 is explained by observations of a weak dependence of ω_0 on intercalate concentration. (A weak dependence of ω_0 on temperature is also found.) The line-shape analysis of Fig. 5 also provides evidence for three weak structures at

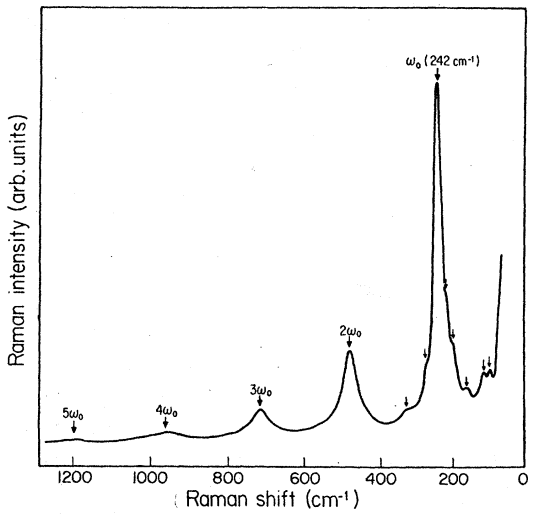

FIG. 4. Raman spectrum for a graphite-bromine compound with 2.7-mole% Br_2 at $T = 77$ K and laser energy 2.54 eV in the frequency region where the intercalate modes are dominant. The structure identified with the Br_2 stretching mode in the intercalation compound is denoted by ω_0, and its harmonics by $n\omega_0$. Fine structure in the vicinity of ω_0 is indicated by arrows.

higher frequencies (see Table II), each upshifted from the fundamental and from each other by ~10 cm^{-1}. In the frequency range in the vicinity of 300 cm^{-1}, broad background scattering is found, probably due to the presence of small regions of solid bromine in the bromine-saturated compound. Below the main peak, a moderately intense peak is found at 230.3 cm^{-1}, as well as two weaker peaks at 213.5 and 198.5 cm^{-1}. These three structures are each downshifted from one another by ~16 cm^{-1}, starting from the 245.4-cm^{-1} structure. In addition, two lines are observed in the vicinity of 100 cm^{-1} (see Table II), corresponding to the band of librational frequencies in solid bromine.[13] The linewidth of the various components at 77 K (see Table II) is ~5 cm^{-1}, which is comparable with the frequency shifts associated with the isotope effect in solid bromine.[13] This suggests that the isotope effects is not resolved in the intercalation compounds and that the fine structure observed for the intercalate modes is not due to isotope effects. It is also of interest that at room temperature the fine structure in Fig. 4 is not resolved, the linewidth associated with the ω_0 structure is greatly increased, and the intensity of the harmonic structure in Fig. 4 is greatly decreased.[7]

Spectra such as those shown in Figs. 4 and 5 are obtained over a wide range of intercalate concentrations. A summary of the peak positions (as denoted in Fig. 4 by arrows) of various spectral

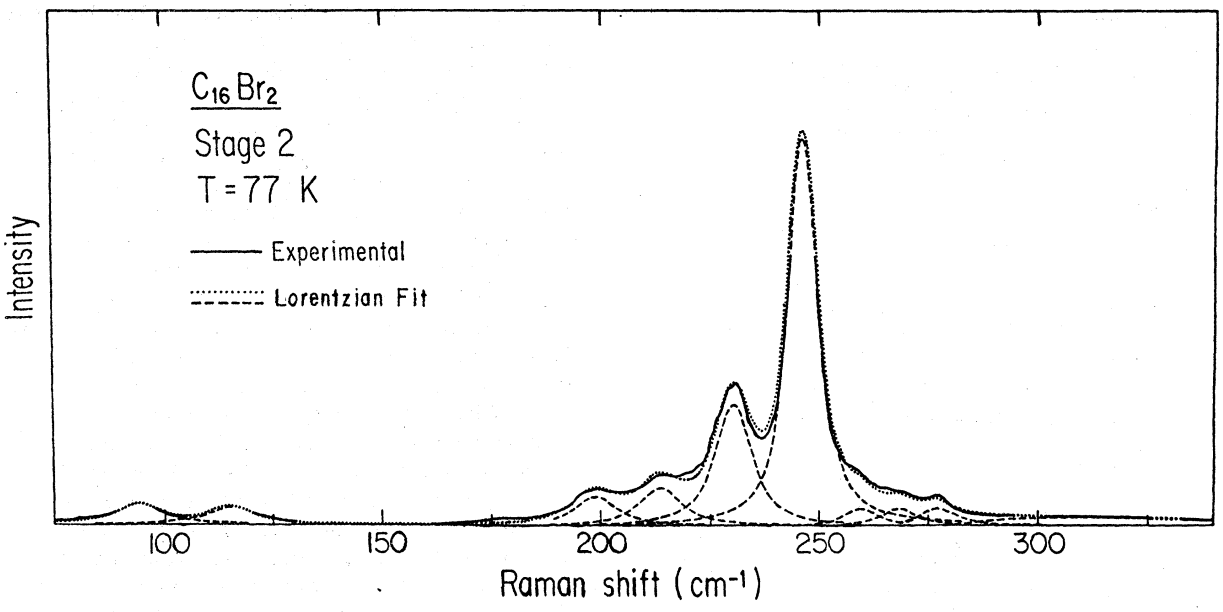

FIG. 5. Expanded view of the Raman spectrum for a $C_{16}Br_2$(stage-2) compound at $T=77$ K and laser energy 2.71 eV between 80 and 300 cm^{-1}. An analysis of the experimental trace (solid curve) into Lorentzian components convolved with the instrument function is shown as the dashed curves and the superposition of the dashed curves appears as the dotted curve. The Lorentzian line-shape parameters for these components are given in Table II.

lines is given in Fig. 6 as a function of intercalate concentration. Also shown in this figure are the stretch and librational modes in solid bromine and the E_{2g_1} and the B_{1g_1} modes of graphite. The ω_0 mode is specially labeled. Of particular significance is the insensitivity of the *frequency* of these lines to bromine concentration, with frequency shifts over the entire range of intercalate concentrations comparable with the linewidths. The observation of the same basic spectrum for very dilute graphite-bromine compounds (e.g., $n=12$ in $C_{8n}Br_2$) is consistent with the observation of similar in-plane electron-diffraction patterns over a wide range of intercalate concentrations, including very dilute concentrations.[5,6,20]

Although the *frequencies* of the intercalate modes in Fig. 6 are relatively insensitive to intercalate concentration, the *intensity* of the intercalate modes increases monotonically with increasing intercalate concentration. Moreover, this intensity increase is at the same rate as the intensity increase of the E_{2g_2} mode in the *bounding* graphite layer denoted by $\hat{E}_{2g_2}$. This result is consistent with the identification of the modes in Fig. 4 with the intercalate species, because the introduction of an intercalate layer is accompanied by the introduction of graphite bounding layers. Furthermore, the intensity of the E_{2g_2} mode for the *interior* graphite layers, denoted by $E^0_{2g_2}$, decreases with increasing intercalate concentration.[7,8,10,11]

TABLE II. Parameters describing Lorentzian components of spectrum in Fig. 5.

Peak frequency (cm^{-1})	Linewidth (cm^{-1})	Intensity (arbitrary units)
310	25	0.1
277	4	0.22
269.5	5	0.15
259	5	0.19
246.5	3	4.45
230.3	4	1.40
213.5	5	0.44
198.5	5	0.34
115.3	5	0.20
94.5	5	0.22

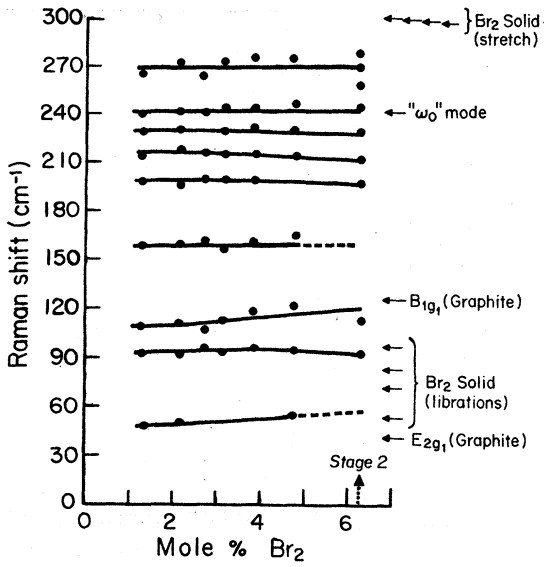

FIG. 6. Dependence of the Raman mode frequencies on intercalate concentration for the low-frequency modes at 77 K (see arrows on Fig. 4). Stage 2 corresponds to 6.25-mole% Br_2. To help with the identification of the low-frequency modes, characteristic frequencies are indicated for the molecular stretch modes and the librational modes in solid bromine, and for the graphite E_{2g_1} and B_{1g_1} modes. The ω_0 mode for the intercalation compound is specially labeled.

In particular, the intensity ratios $I(\hat{E}_{2g_2})/I(E^0_{2g_2})$ and $I(\omega_0)/I(E^0_{2g_2})$ scale as a function of intercalate concentration.

Strong support for the identification of the spectrum in Fig. 4 with intercalate modes also comes from the dependence of this spectrum on laser excitation energy. These data are presented in Fig. 7 by plotting $I(\omega_0)/I(\hat{E}_{2g_2})$ versus laser energy. A logarithmic (base e) scale is chosen for the intensity axis because of the 2 or 3 orders-of-magnitude increase in the intensity ratio over the laser energy range $1.9 < \hbar\omega < 2.7$ eV. We attribute this large increase in intensity to a resonant Raman effect arising from the resonance of the laser excitation with electronic transitions.[24,25]

The intercalate intensity $I(\omega_0)$ in Fig. 7 is normalized to that of the graphite bounding layers $I(\hat{E}_{2g_2})$ for several reasons. Firstly, at a fixed laser excitation energy, this ratio is independent of intercalate concentration. Secondly, with this normalization, the effect of laser energy-dependent corrections for the instrument function is minimized. Furthermore, the ratio of the graphite bounding layer intensity $I(\hat{E}_{2g_2})$ to that of the interior graphite layers $I(E^0_{2g_2})$ is independent of laser excitation energy in this energy range, as shown in Fig. 7 for two intercalate concentrations ($C_{8n}Br_2$, $n = 5, 12$). We thus conclude that the laser energy dependence of $I(\omega_0)/I(\hat{E}_{2g_2})$ is associated with the intercalate ω_0 mode. Also of interest is the observation that the laser energy dependence of $I(\omega_0)/I(\hat{E}_{2g_2})$ is not sensitive to intercalate concentration over a wide range of concentrations.

The strong dependence of $I(\omega_0)$ on laser excitation energy is interpreted in terms of a resonant enhancement effect due to bromine electronic states because of the following arguments. Since the ω_0 mode is associated with a bromine lattice mode, its resonant enhancement is likewise associated with an electronic bromine level. Moreover, the absence of a laser energy dependence of $I(\hat{E}_{2g_2})/I(E^0_{2g_2})$ is consistent with the identification of these modes with vibrations in the graphite layers because of the absence of structure due to electronic transitions in the optical reflectivity of pristine graphite in the photon energy range relevant to Fig. 7. The principal electronic transition in graphite is at ~5 eV and is associated with transitions between π and σ bands; a weaker transition between π bands is also observed near 0.8 eV in pristine graphite.[26] On the other hand, electronic transitions for the free Br_2 molecule are observed at 1.713 eV and an ionization continuum is found above 1.971 eV.[14] The corresponding transitions in solid bromine and in the graphite-bromine intercalation compounds have not yet been reported. The data of Fig. 7 cover 2 to 3 orders of magnitude on the intensity scale; however, no peak in the resonant enhancement curve was found for the

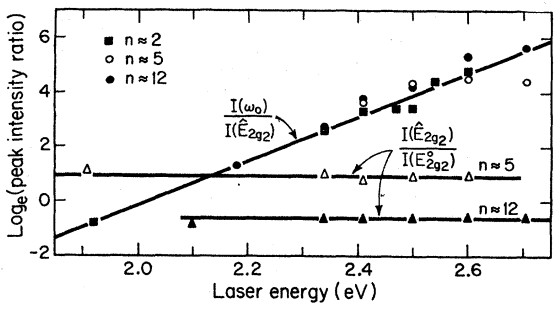

FIG. 7. Dependence of Raman peak intensities on laser excitation energy for $C_{8n}Br_2$ compounds (n being the stage) of several intercalate concentrations. The intensity ratio for the $\hat{E}_{2g_2}$ mode on the graphite bounding layer compared with that for the $E^0_{2g_2}$ mode in the graphite interior layers, denoted by $I(\hat{E}_{2g_2})/I(E^0_{2g_2})$, is independent of laser energy, but dependent on bromine intercalate concentration. In contrast, the intensity of the molecular stretch mode ω_0 (as well as the fine structure of Fig. 4) shows large resonant enhancement effects, but has the same dependence on intercalate concentration as the $\hat{E}_{2g_2}$ mode on the graphite bounding layer. The intensity scale is logarithmic (base e) to cover the 2 or 3 orders-of-magnitude increase in $I(\omega_0)/I(\hat{E}_{2g_2})$ in this range of laser energies.

range of available photon energies (up to 2.7 eV), indicating that the electronic transitions responsible for the resonant enhancement are higher in energy than the electronic ionizing transition in the free bromine molecule. Since the addition of bromine increases the free-carrier concentration of graphite bromine, a shift is expected to be most important at high intercalate concentrations. We thus interpret the insensitivity of the resonant enhancement curve to intercalate concentration to indicate that the electronic transition in the intercalation compound is not from a bromine intercalate level to the Fermi level, but is more likely an ionizing transition to a molecular state above the Fermi level. An energy shift of 1 eV for this bromine transition between the gas phase and the intercalation compound is consistent with observations of relaxation polarization shifts in the molecular levels of a variety of adsorbed species.[27]

Of possible relevance to the electronic transitions responsible for the resonant Raman effects observed in the graphite-bromine compounds is the feature in the photoelectron-yield curve identified with a $4p$ bromine level 5 eV below the Fermi level in graphite-bromine compounds using XPS techniques.[28]

While the present work suggests that the resonant Raman effect is associated with transitions between brominelike levels, a detailed discussion of this effect awaits further clarification of the location of the electronic states away from the Fermi level in the graphite-bromine compounds. The observation of a large resonant Raman effect suggests electronic transitions in the graphite-bromine intercalation compounds above 2.7 eV. The relative insensitivity of the resonant enhancement data to intercalate concentration also suggests a weak dependence of these electronic transitions on intercalate concentration.

Thus, through the resonant Raman effect, Raman spectroscopy provides useful information on the electronic levels[24] in graphite intercalation compounds. This resonant enhancement phenomena also suggests that by using laser excitation energies near expected or observed intercalate electronic transitions, it may be possible to study the intercalate lattice modes for a variety of intercalate species.

Because of the specificity of the spectra in Fig. 4 to the intercalate species bromine, and because of the observed dependence of these features on intercalate concentration and laser excitation energy, the identification of the spectral lines in Fig. 4 with intercalate modes is well established.

Evidence in support of the molecular identity of the intercalate as predominantly Br_2 (e.g., not Br_2^-) is less well established and is based on the following arguments. From the interpretation of x-ray and electron-diffraction patterns[5,6] the nearest Br-Br distance in the intercalation compound is the same as the intramolecular distance in the gas phase, thereby providing strong evidence for the presence of Br_2 in the graphite-bromine compounds. This conclusion is supported by the interpretation of the magnetoreflection experiments[1] to indicate that the amount of charge transfer to the interior graphite layers is very small (≈ 1 charge per 10^2 bromine intercalate atoms). From the magnetoreflection experiments we conclude that either the bromine intercalate is very weakly ionized, or that, if there is strong ionization, the charge transfer is made to the bounding graphite layers. Hall-effect measurements[2] indicate that these charges are not mobile, since the dependence of the Hall coefficient on intercalate concentration is consistent with a low carrier concentration relative to the intercalate concentration.[1,2] A small carrier concentration is also consistent with the location of the plasma frequency for graphite-bromine compounds in the near infrared.[4,22]

These conclusions, based on a variety of other types of experiments, are consistent with the identification of the dominant ω_0 feature of the Raman spectra in Fig. 4 as a Br_2 molecular stretch mode,[7] though this mode is downshifted from the molecular stretch mode in solid bromine by 58 cm^{-1}. The close correspondence of the nearest-neighbor intermolecular distance in the bromine intercalate layer[5,6] and in solid bromine[15] (a solid of Van der Waals–bonded Br_2 molecules) also strongly supports the dominance of the Br_2 species in the intercalation compound and the identification of the ω_0 structure in Fig. 4 with the Br_2 stretch modes. Figures 4 and 5, however, show a collection of weaker Raman lines. Since the carrier concentration increases with increasing bromine concentration, it is reasonable to assume that some fraction of the bromine intercalate is ionized, and this ionized species (e.g., Br_2^-) could give rise to additional spectral lines. Furthermore the discussion in Sec. II indicates that the ordering of the bromine molecular axes in the intercalate layer gives rise to a multiplicity of molecular stretch modes, depending on the particular molecular arrangement. These various stretch modes are expected to have approximately the same frequency. It is suggested that the cluster of modes about ω_0 in Fig. 5 is associated with these multiple molecular stretch modes and with the simultaneous presence of domains exhibiting different molecular alignment arrangements. An identification of the two low-frequency modes with librational motions is suggested by the correspondence of these mode frequencies with librational

modes in solid Br_2. To carry out a detailed identification of the variety of intercalate modes shown in Fig. 5, careful polarization studies will have to be carried out on carefully prepared, well-annealed single-phase samples. In this connection, the symmetry analysis presented in Sec. II for some likely types of molecular arrangements will be useful. Such polarization studies are now in progress. In this work particular attention is being given to the temperature dependence of the spectra as a means for identifying order-disorder transformations in graphite-bromine compounds, as suggested by x-ray and electron-diffraction studies.

ACKNOWLEDGMENTS

The authors would like to thank Dr. D. D. L. Chung and Dr. J. J. Song for their contributions to the early phases of this research. The authors also appreciate valuable discussions with B. L. Heflinger, C.-L. Lau and Dr. C. Underhill. This work has been supported by the ONR Grant No. N00014-77-C-0053.

---

*Center for Materials Science and Engineering, and Dept. of Electrical Engineering and Computer Science.
†Visiting Scientist, Francis Bitter National Magnet Laboratory, sponsored by the NSF.
‡Now at Physics Dept., University of Kentucky, Lexington, Kentucky.
§Francis Bitter National Magnet Laboratory, sponsored by the NSF.

[1]D. A. Platts, D. D. L. Chung, and M. S. Dresselhaus, Phys. Rev. B 15, 1087 (1977).
[2]G. R. Hennig, J. Chem. Phys. 20, 1443 (1952).
[3]G. Dresselhaus and M. S. Dresselhaus, Mater. Sci. Eng. 31, 235 (1977).
[4]R. A. Wachnik, B. S. thesis (MIT, Cambridge, MA, 1977) (unpublished).
[5]W. T. Eeles and J. A. Turnbull, Proc. R. Soc. A 283, 179 (1965).
[6]J. A. Turnbull and W. T. Eeles, in Second Conference on Industrial Carbon and Graphite (Society of Chemical Industries, London, 1966), p. 173.
[7]J. J. Song, D. D. L. Chung, P. C. Eklund, and M. S. Dresselhaus, Solid State Commun. 20, 1111 (1976).
[8]R. G. Nemanich, S. A. Solin, and D. Guerard, Phys. Rev. B 16, 2965 (1977).
[9]P. C. Eklund, G. Dresselhaus, M. S. Dresselhaus, and J. E. Fischer, Phys. Rev. B 15, 3180 (1977).
[10]M. S. Dresselhaus, G. Dresselhaus, P. C. Eklund, and D. D. L. Chung, Mater. Sci. Eng. 31, 141 (1977).
[11]S. A. Solin, Mater. Sci. Eng. 31, 153 (1977).
[12]Several recent references have appeared on the subject of lattice modes in pristine graphite with particular reference to out-of-plane modes and second-order Raman spectra for in-plane modes: R. J. Nemanich, G. Lucovsky, and S. A. Solin, Solid State Commun. 23, 117 (1977); R. J. Nemanich and S. A. Solin, *ibid.* 23, 417 (1977); R. J. Nemanich, G. Lucovsky and S. A. Solin, Mater. Sci. Eng. 31, 157 (1977).
[13]J. E. Cahill and G. E. Leroi, J. Chem. Phys. 51, 4514 (1966).
[14]G. Herzberg, Spectra of Diatomic Molecules, 2nd ed. (Van Nostrand, New York, 1948), Vol. 1, p. 368.
[15]R. W. G. Wyckoff, Crystal Structures, 2nd ed. (Interscience, New York, 1948), Vol. 1, p. 52.
[16]W. Rüdorff and E. Schulze, Z. Anorg. Allg. Chem. 277, 156 (1954).
[17]W. Rüdorff, Z. Anorg. Allg. Chem. 245, 383 (1941).
[18]L. C. F. Blackman, J. F. Mathews, and A. R. Ubbelohde, Proc. R. Soc. A 256, 15 (1960).
[19]J. E. Fischer, Mater. Sci. Eng. 31, 211 (1977).
[20]D. D. L. Chung, Ph.D. thesis (MIT, Cambridge, MA., 1977) (unpublished).
[21]G. A. Saunders, A. R. Ubbelohde, and D. A. Young, Proc. R. Soc. A 271, 499 (1963).
[22]G. R. Hennig, J. Chem. Phys. 20, 1438 (1952).
[23]T. Sasa, Y. Takahashi and T. Mukaibo, Carbon 9, 407 (1971).
[24]R. Loudon, Adv. Phys. 13, 423 (1964); J. Phys. 26, 677 (1965).
[25]R. C. C. Leite and S. P. S. Porto, Phys. Rev. Lett. 17, 10 (1966).
[26]E. A. Taft and H. R. Philipp, Phys. Rev. A 197, 138 (1965).
[27]G. N. Rubloff, W. D. Grobman, and H. Lüth, Phys. Rev. B 14, 1450 (1976).
[28]B. Bach, E. Ll. Evans, J. M. Thomas, and M. Barber, Chem. Phys. Lett. 10, 547 (1971).